UNSYS digital

Motion Analysis of Intermeshing Quadrotor Helicopter

Satoshi Suzuki, Yohei Fujisawa, Mikio Nakamura, Kojiro Iizuka, Takashi Kawamura

Shinshu University, Japan

Abstract— In this study, we propose an intermeshing quadrotor helicopter which has both characteristics of a tandem-rotor helicopter and an intermeshing-rotor helicopter. The helicopter has well longitudinal stability properties like the tandem-rotor helicopter and well lateral stability property like the intermeshing-rotor helicopter. The energy conversion efficiency of proposed helicopter is better than which of single-rotor helicopters. However, there are several unknown parts about its motion characteristics because such a helicopter has not existed so far. Therefore, it is necessary to conduct the motion analysis of the helicopter. In this paper, the mathematical model of intermeshing quadrotor helicopter is derived to perform fundamental motion analysis by using multi body dynamics technique.

Keywords—Intermeshing quadrotor helicopter, modeling, motion analysis.

I. INTRODUCTION

IN recent years, unmanned helicopter has become to be developed and used for various practical purposes such as aerial photography, surveillance, and crop dusting. Unmanned helicopters are safer and more convenient than manned helicopters, and they can be potentially employed in a wide range of applications. There are many types of unmanned helicopter, which have various sizes, weights, and have various mechanisms. For example, there are single-rotor type, co-axial rotor type, tandem rotor type, and multi rotor type (quad rotor or more) helicopter which are presented [1]-[4]. In this study, we are focusing our interests on counter rotating type helicopter, such as co-axial rotor, tandem-rotor, and intermeshing-rotor type helicopter. The energy conversion efficiency of these kinds of helicopters is better than those of the single rotor helicopter because such helicopters have no tail rotor. The tandem rotor type helicopter can locate its center of gravity widely back and forth, and has good longitudinal operational stability. Therefore, tandem rotor helicopter is widely used for transportation. On the other hand, the intermeshing rotor type helicopter has good lateral operational stability, and has outstanding stability property in the case when there are heavy loads between two rotors. Thus, the intermeshing rotor helicopter is suited to lifting of heavy goods such as an aerial crane. Combining these good characteristics of tandem rotor and intermeshing rotor helicopter, we propose intermeshing quadrotor helicopter shown in **Figure 1**. This helicopter seems to have good lateral and longitudinal stability, and has good energy conversion efficiency. However, there are several unknown parts about its motion characteristics because such a helicopter has not existed so far. Therefore, it is necessary to conduct the motion analysis of the helicopter. In this paper, the mathematical model of the intermeshing quadrotor helicopter, which is used for the motion analysis of the helicopter, is derived by using multi-body dynamics modeling technique. *Velocity transformation method* is used to derive equation of motion of the helicopter including rotor flapping motion. All the forces and moments generated by rotors are derived in consideration of rotor aerodynamics. The flight experiment is carried out to collect the flight data for identification of the model parameters.

Figure 1 Intermeshing quadrotor helicopter.

The rest of this paper is organized as follows. The intermeshing quad rotor helicopter is introduced in Section II. The equation of motion of the helicopter is derived in Section III, then force and torque terms generated by intermeshing rotors are also derived. In Section IV, the control system for flight experiment is designed and developed. Flight experiment for data collection is performed by using designed control system. Finally, the conclusion of this work is shown in section V.

II. INTERMESHING QUADROTOR HELICOPTER

The main specifications of the intermeshing quadrotor helicopter are listed in **TABLE I**. The source of the power of this helicopter is hobby-used glow engine, and driving torque generated by the engine is transferred to two couples of intermeshing rotors by drive shaft mechanism. Therefore, the four rotors could rotate as the same rotational speed. The overview of the drive shaft mechanism is shown in **Figure 2**. Additionally, the helicopter equips four servo motors in the bottom of each rotor, and blade collective pitch angle of the each rotor could be actuated individually by using the servo motor (**Figure 3**). Change of the collective pitch angle of the

Corresponding author: Satoshi Suzuki (e-mail: s-s-2208@shinshu-u.ac.jp).
This paper was submitted on November 28, 2013; revised on March 7, 2014; and accepted on April 3, 2014.

rotor provides the change of the rotor thrust, and then three axis forces are generated by rotor thrust, and moments are generated by using rotor thrust differentials. There are several differences between the intermeshing quadrotor helicopter and regular quadrotor helicopter presented in [4]. The differences between two quadrotor helicopters are summarized in **TABLE II**.

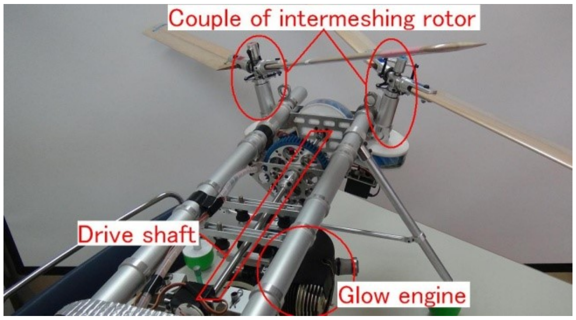

Figure 2 Drive shaft mechanism.

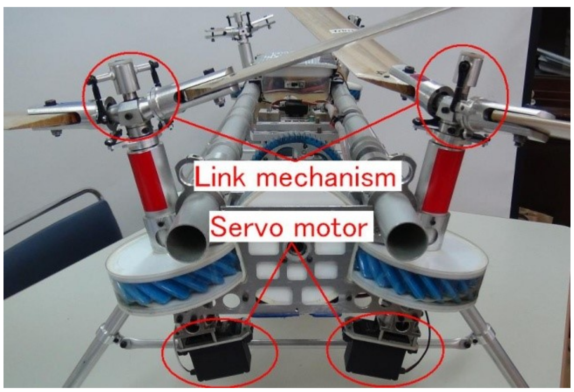

Figure 3 Collective pitch mechanism.

TABLE I
Main specifications of intermeshing quadrotor helicopter

Source of power	Glow engine
Rotor diameter	820 mm
Body length (without rotor)	850 mm
Body width (without rotor)	210 mm
Rotor speed	1700-1900 rpm
Weight	6.4 kg
Inclination angle of the rotor	12 deg

TABLE II
Differences between regular and intermeshing quadrotor helicopter

Items	Regular	Intermeshing
Revolution of the rotors	Individual	Synchronized
Rotor arrangement	Planar	Non-planer
Blade pitch	Fixed	Variable (only collective pitch)
Control input	Rotor revolution	Collective pitch

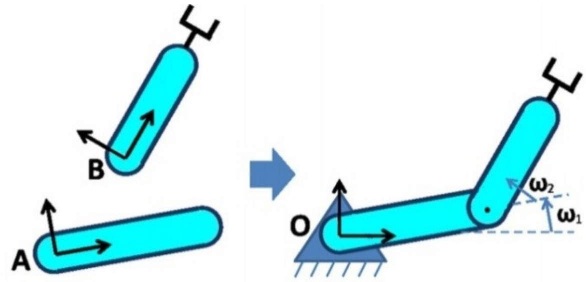

Figure 4 Basic concepts of velocity transformation method.

III. MODELING OF INTERMESHING QUADROTOR HELICOPTER

In this section, the mathematical model of the intermeshing quadrotor helicopter is derived. We consider the helicopter as a rigid model which consists of five rigid bodies: fuselage and four rotors. By considering the four rotors as individual rigid bodies, the mathematical model could include the flapping dynamics of the rotor which is the most important part in the dynamics of the helicopter. To derive the equation of motion of the helicopter, multi-body dynamics technique is used. First, we introduce the velocity transformation method, which is one of multi-body dynamics technique. Next, we apply this method to intermeshing quadrotor helicopter, and the nonlinear equation of motion is derived.

A. Velocity Transformation method

The velocity transformation method is one of the multi-body dynamics technique proposed by Tajima [5], and it is similar to a traditional velocity transformation technique. The detail of the method is presented in [5], and the details of the velocity transformation technique also appear [6]-[8]. In the following, we introduce the outline of the velocity transformation method by using **Figure 4**. In **Figure 4**, two-link robotic manipulator which consists of link A, link B, and pin joint is defined.

First, the generalized velocity of rigid bodies without constraints is considered as $\boldsymbol{H}$. $\boldsymbol{H}$ consists of linear and rotational velocity of each link such as

$$\mathbf{H} = \begin{bmatrix} \mathbf{V}_{\mathbf{A}}^T & \boldsymbol{\Omega}_{\mathbf{A}}^T & \mathbf{V}_{\mathbf{B}}^T & \boldsymbol{\Omega}_{\mathbf{B}}^T \end{bmatrix}^T \tag{1}$$

Then the equation of motion of the link system without constraints is obtained as

$$\boldsymbol{m}^H \dot{\boldsymbol{H}} = \boldsymbol{f}^H \tag{2}$$

Here, $\boldsymbol{m}^H$ is a symmetric matrix representing the inertia of the rigid bodies, $\boldsymbol{f}^H$ is the external force which is impressed on the rigid bodies. Now, the constrains by pin joint is added to the link system, (2) is rewritten as

$$\boldsymbol{m}^H \dot{\boldsymbol{H}} = \boldsymbol{f}^H + \bar{\boldsymbol{f}}^H \tag{3}$$

Here, $\bar{\boldsymbol{f}}^H$ represents the constraint force by pin joints. On the other hand, a generalized velocity of the link system with constraints is considered as $\boldsymbol{S}$. In this case, $\boldsymbol{S}$ includes the angular velocity of each link around the pin joint as follows:

$$\boldsymbol{S} = [\omega_1 \quad \omega_2]^T \tag{4}$$

And the equation of the motion with constraints is obtained as

$$\boldsymbol{m}^S \dot{\boldsymbol{S}} = \boldsymbol{f}^S \quad (5)$$

Here, $\boldsymbol{m}^S$ represents the inertia matrix, and $\boldsymbol{f}^S$ represents the external force vector. Now, in the case of holonomic and simple non-holonomic system, the relation between generalized velocities $\boldsymbol{H}$ and $\boldsymbol{S}$ is obtained as follows:

$$\boldsymbol{H} = \boldsymbol{H}_S \boldsymbol{S} + \boldsymbol{H}_{\bar{S}} \quad (6)$$

Here, $\boldsymbol{H}_S$ and $\boldsymbol{H}_{\bar{S}}$ are appropriate matrices. Calculating the time derivatives of (6), and substituting it into (2), the next equation could be obtained

$$\boldsymbol{H}_S^T \boldsymbol{m}^H \boldsymbol{H}_S \dot{\boldsymbol{S}} = \boldsymbol{H}_S^T \left\{ \boldsymbol{f}^H - \boldsymbol{m}^H \left(\frac{d\boldsymbol{H}_S}{dt} \boldsymbol{S} + \frac{d\boldsymbol{H}_{\bar{S}}}{dt} \right) + \bar{\boldsymbol{f}}^H \right\} \quad (7)$$

According to [5], it can be easily shown that $\boldsymbol{H}_S^T \bar{\boldsymbol{f}}^H$ is equal to zero. Therefore, comparing (5) and (7), $\boldsymbol{m}^S$ and $\boldsymbol{f}^S$ could be expressed by using $\boldsymbol{m}^H$ and $\boldsymbol{f}^H$ as follows:

$$\boldsymbol{m}^S = \boldsymbol{H}_S^T \boldsymbol{m}^H \boldsymbol{H}_S \quad (8)$$

$$\boldsymbol{f}^S = \boldsymbol{H}_S^T \left\{ \boldsymbol{f}^H - \boldsymbol{m}^H \left(\frac{d\boldsymbol{H}_S}{dt} \boldsymbol{S} + \frac{d\boldsymbol{H}_{\bar{S}}}{dt} \right) \right\} \quad (9)$$

If $\boldsymbol{m}^H$ and $\boldsymbol{f}^H$ were given and the relation (6) could be derived, the equation of motion of two-link robotic manipulator could be obtained by using (5), (8), and (9). This method includes the velocity transformation (6) that the method is called velocity transformation method.

B. Equation of Motion of intermeshing quadrotor helicopter

The equation of motion of the intermeshing quadrotor helicopter is derived by using the velocity transformation method. First, coordinate systems used in this section are defined in **Figure 5**. $\boldsymbol{O}$ is inertial frame fixed at ground, $\boldsymbol{B}$ is body frame fixed at the center of gravity of the helicopter, and $\boldsymbol{r_1}$-$\boldsymbol{r_4}$ is rotor frame fixed at the center of each rotor blade. $\boldsymbol{B}$ moves in conjunction with the motion of the fuselage, and $\boldsymbol{r_1}$-$\boldsymbol{r_4}$ move in conjunction with the rotation of each rotor blade. Moreover, $\boldsymbol{R_{OB}}$ represents the position of the origin of $\boldsymbol{B}$ relative to the origin of $\boldsymbol{O}$, and it is expressed as the vector on $\boldsymbol{O}$. On the other hand, $\boldsymbol{R'_{OB}}$ represents the same vector which is expressed on $\boldsymbol{B}$. This manner is also applied to linear velocity, angular velocity, forces and torque vector.

Now, equation of motion without constraints is derived. If there were no constraints between the fuselage and each rotor blade, the fuselage and each rotor blade are regarded as free rigid bodies. Thus, the equation of motion of each rigid body is represented as follows:

$$\boldsymbol{M_B \dot{V}'_{OB}} = \boldsymbol{F'_{OB}} - \boldsymbol{M_B \tilde{\Omega}'_{OB} V'_{OB}} \quad (10)$$

$$\boldsymbol{J_B \dot{\Omega}'_{OB}} = \boldsymbol{N'_{OB}} - \boldsymbol{\tilde{\Omega}'_{OB} J_B \Omega'_{OB}} \quad (11)$$

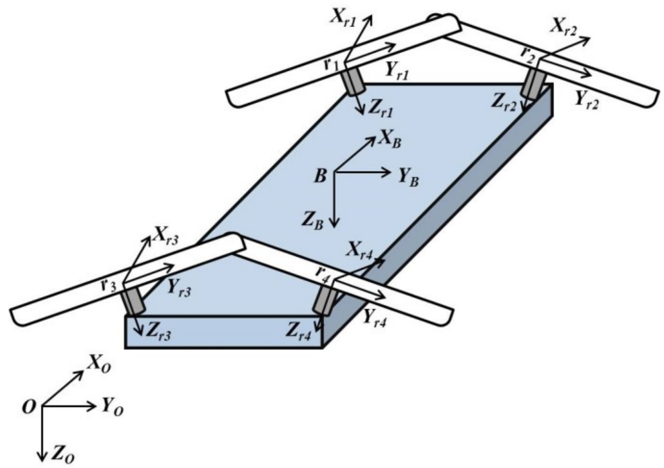

Figure 5 Coordinate systems.

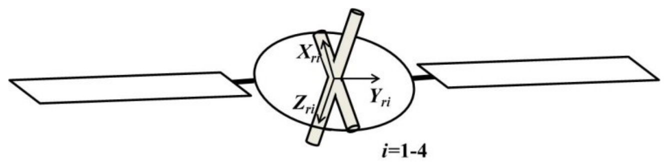

Figure 6 Kinematic constraint of rotor blade.

$$\boldsymbol{M_i \dot{V}'_{Ori}} = \boldsymbol{F'_{Ori}} - \boldsymbol{M_{ri} \tilde{\Omega}'_{Ori} V'_{Ori}} \qquad (\boldsymbol{i} = 1,2,3,4) \quad (12)$$

$$\boldsymbol{M_{ri} \dot{V}'_{Ori}} = \boldsymbol{F'_{Ori}} - \boldsymbol{M_{ri} \tilde{\Omega}'_{Ori} V'_{Ori}} \qquad (\boldsymbol{i} = 1,2,3,4) \quad (13)$$

Here, $\boldsymbol{M}$ denotes the mass of the unit, $\boldsymbol{J}$, the inertia matrix, $\boldsymbol{V}$ and $\boldsymbol{\Omega}$, the linear and angular velocity, and $\boldsymbol{F}$, $\boldsymbol{N}$ denote the external force and torque vector. Additionally, $\boldsymbol{\tilde{\Omega}'}$ denotes the skew symmetric matrix which represents vector product. Now, we choose the generalized velocity without constraints as

$$\boldsymbol{H} = \begin{bmatrix} V'^T_{OB} & \Omega'^T_{OB} & V'^T_{Or1} & \Omega'^T_{Or1} & V'^T_{Or2} & \Omega'^T_{Or2} & V'^T_{Or3} & \Omega'^T_{Or3} & V'^T_{Or4} & \Omega'^T_{Or4} \end{bmatrix}^T \quad (14)$$

Then, $\boldsymbol{m}^H$ and $\boldsymbol{f}^H$ in (2) are obtained from (10)-(13) as

$$\mathbf{m}^H = diag\left(\mathbf{M_B} \quad \mathbf{J_B} \quad \mathbf{M_{r1}} \quad \mathbf{J_{r1}} \quad \mathbf{M_{r2}} \quad \mathbf{J_{r2}} \quad \mathbf{M_{r3}} \quad \mathbf{J_{r3}} \quad \mathbf{M_{r4}} \quad \mathbf{J_{r4}}\right) \quad (15)$$

$$\mathbf{f}^H = \begin{bmatrix} \mathbf{F'_{OB}} - \mathbf{M_B \tilde{\Omega}'_{OB} V'_{OB}} \\ \mathbf{N'_{OB}} - \mathbf{\tilde{\Omega}'_{OB} J_B \Omega'_{OB}} \\ \mathbf{F'_{Or1}} - \mathbf{M_{r1} \tilde{\Omega}'_{Or1} V'_{Or1}} \\ \mathbf{N'_{Or1}} - \mathbf{\tilde{\Omega}'_{Or1} J_{r1} \Omega'_{Or1}} \\ \mathbf{F'_{Or2}} - \mathbf{M_{r2} \tilde{\Omega}'_{Or2} V'_{Or2}} \\ \mathbf{N'_{Or2}} - \mathbf{\tilde{\Omega}'_{Or2} J_{r2} \Omega'_{Or2}} \\ \mathbf{F'_{Or3}} - \mathbf{M_{r3} \tilde{\Omega}'_{Or3} V'_{Or3}} \\ \mathbf{N'_{Or3}} - \mathbf{\tilde{\Omega}'_{Or3} J_{r3} \Omega'_{Or3}} \\ \mathbf{F'_{Or4}} - \mathbf{M_{r4} \tilde{\Omega}'_{Or4} V'_{Or4}} \\ \mathbf{N'_{Or4}} - \mathbf{\tilde{\Omega}'_{Or4} J_{r4} \Omega'_{Or4}} \end{bmatrix} \quad (16)$$

Next, kinematic constraints are added between the fuselage and each rotor. Now, we assume that each rotor blade connect to the fuselage by the universal joint as shown in **Figure 6**. In **Figure 6** the rotor blade could rotate around $\boldsymbol{X_{ri}}$ and $\boldsymbol{Z_{ri}}$ axis. Additionally, the blade rotates around $\boldsymbol{Z_{ri}}$ axis as angular velocity Ω. Then, position constraints of each rotor could be expressed as follows:

$$\boldsymbol{R_{Ori}} = \boldsymbol{R_{OB}} + \boldsymbol{C_{OB}}\boldsymbol{R_{Bri}} \qquad (\boldsymbol{i} = 1,2,3,4) \qquad (17)$$

Here, $\boldsymbol{C_{OB}}$ is the rotation matrix which represents the coordinate transformation from $\boldsymbol{B}$ to $\boldsymbol{O}$. $\boldsymbol{R_{Bri}}$ represents the position of the center of the rotor blade relative to the origin of $\boldsymbol{B}$, and it is determined by the arrangement of each rotor. Differentiating (17), constraints of linear velocity could be obtained as

$$\boldsymbol{V_{Ori}} = \boldsymbol{V_{OB}} - \boldsymbol{C_{OB}}\widetilde{\boldsymbol{R}}_{\boldsymbol{Bri}}\boldsymbol{\Omega}'_{\boldsymbol{OB}} \qquad (\boldsymbol{i} = 1,2,3,4) \qquad (18)$$

Here, time derivatives of $\boldsymbol{R_{Bri}}$ is zero because the components of $\boldsymbol{R_{Bri}}$ are constant. Similarly, the constraints of $\boldsymbol{V'_{Ori}}$ could be obtained as

$$\boldsymbol{V'_{Ori}} = \boldsymbol{C_{riB}}\boldsymbol{V'_{OB}} - \boldsymbol{C_{riB}}\widetilde{\boldsymbol{R}}_{\boldsymbol{Bri}}\boldsymbol{\Omega}'_{\boldsymbol{OB}} \qquad (\boldsymbol{i} = 1,2,3,4) \qquad (19)$$

Next, the constraints of angular velocity are derived. Considering the blade flapping angle of each rotor as $\beta_{\boldsymbol{ri}}\ (\boldsymbol{i} = 1-4)$, the constraints of angular velocity are obtained as

$$\boldsymbol{\Omega'_{Ori}} = \begin{bmatrix}1\\0\\0\end{bmatrix}\dot{\boldsymbol{\beta}}_{\boldsymbol{ri}} + \begin{bmatrix}0\\0\\1\end{bmatrix}\Omega + \boldsymbol{C_{riB}}\boldsymbol{\Omega}'_{OB} \qquad (\boldsymbol{i} = 1,2,3,4) \qquad (20)$$

Now, we define the generalized velocity with kinematic constraints $\boldsymbol{S}$ by using linear and angular velocity of the fuselage, and flapping angular velocity of each rotor as

$$\boldsymbol{S} = \begin{bmatrix}\boldsymbol{V}'^T_{\boldsymbol{OB}} & \boldsymbol{\Omega}'^T_{\boldsymbol{OB}} & \dot{\beta}_{r1} & \dot{\beta}_{r2} & \dot{\beta}_{r3} & \dot{\beta}_{r4}\end{bmatrix}^T \qquad (21)$$

Using (14), (19), (20), and (21), $\boldsymbol{H}_S$ and $\boldsymbol{H}_{\bar{S}}$ in (6) could be obtained as follows

$$\boldsymbol{H}_S = \begin{bmatrix}\boldsymbol{I} & \boldsymbol{0} & \boldsymbol{0} & \boldsymbol{0} & \boldsymbol{0}\\ \boldsymbol{0} & \boldsymbol{I} & \boldsymbol{0} & \boldsymbol{0} & \boldsymbol{0}\\ \boldsymbol{C}_{r1B} & -\boldsymbol{C}_{r1B}\widetilde{\boldsymbol{R}}_{Br1} & \boldsymbol{0} & \boldsymbol{0} & \boldsymbol{0}\\ \boldsymbol{0} & \boldsymbol{C}_{r1B} & \boldsymbol{0} & \boldsymbol{E}_x & \boldsymbol{0}\\ \boldsymbol{C}_{r2B} & -\boldsymbol{C}_{r2B}\widetilde{\boldsymbol{R}}_{Br2} & \boldsymbol{0} & \boldsymbol{0} & \boldsymbol{0}\\ \boldsymbol{0} & \boldsymbol{C}_{r2B} & \boldsymbol{0} & \boldsymbol{E}_x & \boldsymbol{0}\\ \boldsymbol{C}_{r3B} & -\boldsymbol{C}_{r3B}\widetilde{\boldsymbol{R}}_{Br3} & \boldsymbol{0} & \boldsymbol{0} & \boldsymbol{0}\\ \boldsymbol{0} & \boldsymbol{C}_{r3B} & \boldsymbol{0} & \boldsymbol{E}_x & \boldsymbol{0}\\ \boldsymbol{C}_{r4B} & -\boldsymbol{C}_{r4B}\widetilde{\boldsymbol{R}}_{Br4} & \boldsymbol{0} & \boldsymbol{0} & \boldsymbol{0}\\ \boldsymbol{0} & \boldsymbol{C}_{r4B} & \boldsymbol{0} & \boldsymbol{E}_x & \boldsymbol{0}\end{bmatrix} \quad \boldsymbol{H}_{\bar{S}} = \begin{bmatrix}\boldsymbol{0}\\ \boldsymbol{0}\\ \boldsymbol{0}\\ \boldsymbol{E}_Z\Omega\\ \boldsymbol{0}\\ \boldsymbol{E}_Z\Omega\\ \boldsymbol{0}\\ \boldsymbol{E}_Z\Omega\\ \boldsymbol{0}\\ \boldsymbol{E}_Z\Omega\end{bmatrix} \qquad (22)$$

Here, $\boldsymbol{E}_x$ and $\boldsymbol{E}_Z$ are defined as

$$\boldsymbol{E_x} = \begin{bmatrix}1 & 0 & 0\end{bmatrix}^T \quad \boldsymbol{E}_Z = \begin{bmatrix}0 & 0 & 1\end{bmatrix}^T \qquad (23)$$

Finally, the equation of motion of intermeshing quadrotor helicopter could be obtained as (5) by using (8), (9), (15), (16), and (22).

C. Derivation of External Forces and Torques

The external force and torque terms in (16) are derived. In flight, aerodynamic forces are applied to the rotor blade. Accordingly, the aerodynamic force and torque generated by the rotors are derived by using rotor aerodynamics. Thrust and torque of each rotor are derived using Blade Element Theory (BET) in **Error! Reference source not found.**. According to BET, the thrust of each rotor in hovering state could be obtained as

$$T_{ri} = \frac{1}{2}\rho a_{ri} c\Omega^2 R_{ri}^3\left(\theta_{tri} + \phi_{tri}\right) \quad (i = 1,2,3,4) \qquad (24)$$

Here, T_{ri} is the thrust generated by each rotor, ρ is the air density, a is lift curve slope of the blade, c is chord length of the blade, R is the radius of the rotor, θ_t and ϕ_t are pitch angle and inflow angle of the blade at blade tip respectively. Similar to the thrust, torque impressed on the rotor blade could be obtained by BET as

$$Q_{ri} = \frac{1}{4}\rho c\Omega^2 R_{ri}^4\left\{C_D - 2a_{ri}\phi_{tri}\left(\theta_{tri} + \phi_{tri}\right)\right\} \quad (i = 1,2,3,4) \qquad (25)$$

Here, Q_{ri} is the torque, C_D is the drag coefficient of the blade.

Additionally, we assume the mechanical constraints shown as **Figure 7** between the rotor and the fuselage to express the stiffness of the rotor blade. Using (24), (25), and **Figure 7**, external forces and torques in (16) could be obtained as follows:

$$\boldsymbol{F'_{OB}} = \boldsymbol{C}^T_{\boldsymbol{OB}}\begin{bmatrix}0\\0\\m_B g\end{bmatrix}$$

$$\boldsymbol{N'_{OB}} = \boldsymbol{C}_{Br1}\begin{bmatrix}k_{r1}\beta_{r1} + c_{r1}\dot{\beta}_{r1}\\0\\0\end{bmatrix} + \boldsymbol{C}_{Br2}\begin{bmatrix}k_{r2}\beta_{r2} + c_{r2}\dot{\beta}_{r2}\\0\\0\end{bmatrix} + \boldsymbol{C}_{Br3}\begin{bmatrix}k_{r3}\beta_{r3} + c_{r3}\dot{\beta}_{r3}\\0\\0\end{bmatrix} + \boldsymbol{C}_{Br4}\begin{bmatrix}k_{r4}\beta_{r4} + c_{r4}\dot{\beta}_{r4}\\0\\0\end{bmatrix} \qquad (26)$$

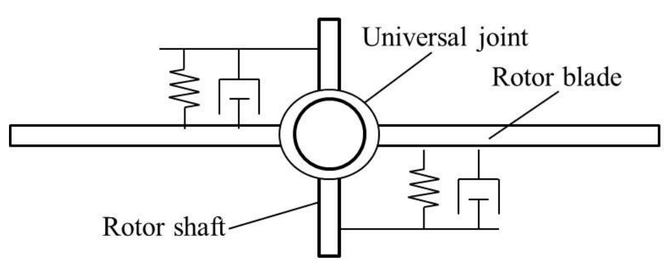

Figure 7 Mechanical constraints of the rotor blade.

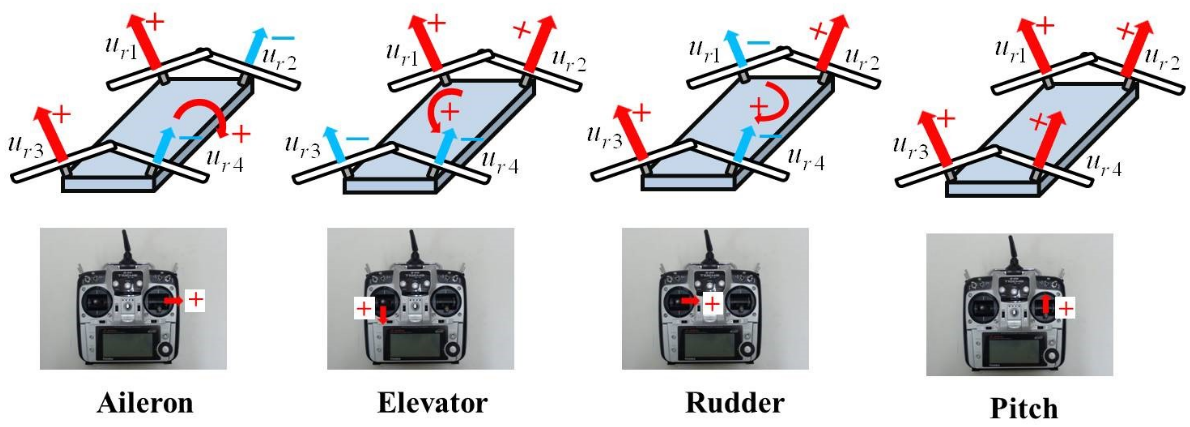

Figure 8 Mixing of control input.

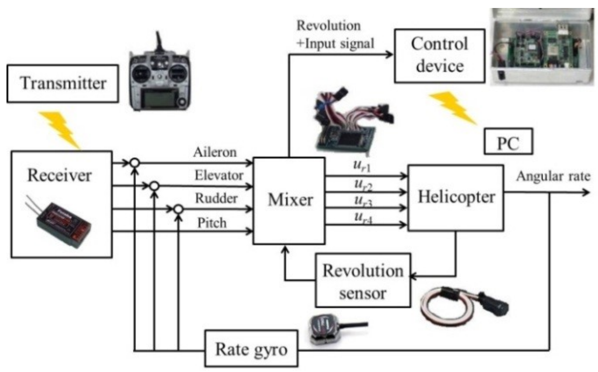

Figure 9 The overview of control system.

$$\boldsymbol{F}_{\boldsymbol{Ori}}^{'} = \boldsymbol{C}_{\boldsymbol{Ori}}^{T}\begin{bmatrix}0\\0\\m_{ri}g\end{bmatrix} + \begin{bmatrix}0\\0\\T_{ri}\end{bmatrix} \quad \boldsymbol{N}_{\boldsymbol{Ori}}^{'} = \begin{bmatrix}-k_{ri}\beta_{ri} - c_{ri}\dot{\beta}_{ri}\\0\\Q_{ri}\end{bmatrix} \quad (i = 1,2,3,4) \tag{27}$$

Here, m is the mass of the fuselage and each rotor, k_{ri} is the spring constant of rotor blade, and c_{ri} is damping coefficient of the blade.

IV. FLIGHT EXPERIMENT

The mathematical model of the intermeshing quadrotor helicopter has several parameters which should be identified by using experimental data. Therefore, flight experiment has to be carried out by manual operation. In this section, the experimental setup for realizing manual flight experiment and the result of the experiment are described.

A. Experimental Setup

The experimental setup is constructed for flight experiment. Figure 8 shows a block diagram of the whole control system for the flight experiment. The system consists of three parts, angular rate feedback by using gyro sensor, mixing of control input, and control device used to measure the state of the helicopter. In the following, the details about angular rate feedback and mixing part are introduced.

First, angular rate feedback part is introduced. There are four operational inputs from the radio transmitter named Aileron, Elevator, Rudder, and Pitch. Aileron is related to the rolling motion of the helicopter, Elevator is related to pitching motion, Rudder is related to yawing motion, and Pitch is related to heave motion (**Figure 9**). If the characteristics of four rotors are completely identical, the helicopter could be operated without any feedback control. However, differences among each rotor blade, the error of the rotor arrangement, and misalignment of the center of gravity always exist. Therefore, the helicopter easily breaks its balance. Moreover, it is extremely difficult to operate the helicopter under wind gust without additional feedback control. To overcome these problems, it is necessary to compensate the operational inputs by using angular rate feedback. Considering the roll, pitch, and yaw angular velocity as p, q, r, the angular rate feedback is obtained as follows:

$$Aileron = Aileron - K_{pr} \cdot p \tag{28}$$

$$Elevator = Elevator - K_{pp} \cdot q \tag{29}$$

$$Rudder = Rudder - K_{py} \cdot r \tag{30}$$

Here, K_{pr}, K_{pp}, and K_{py} are the proportional gain for each axis. We implement such angular rate feedback by using rate gyro system.

Next, mixing part is introduced. In the case of intermeshing quadrotor helicopter, operational input from radio transmitter should be converted to the inputs for four servo motors which are related to the blade collective pitch angle. Now, considering the inputs for servo motor of each rotor as u_{r1}- u_{r4}, relation between the inputs from the transmitter and the inputs for servo motor could be obtained by using **Figure 9** as

$$u_{r1} = +Aileron + Elevator - Rudder + Pitch \tag{31}$$

$$u_{r2} = -Aileron + Elevator + Rudder + Pitch \tag{32}$$

$$u_{r3} = +Aileron - Elevator + Rudder + Pitch \tag{33}$$

$$u_{r4} = -Aileron - Elevator - Rudder + Pitch \tag{34}$$

To realize the input mixing as derived in (31) -**Error! Reference source not found.**, it is better to use logic circuit rather than the software programs because the mixing part requires high reliability for safe flight. However, the modification is not as easy for the logic circuit as the software program. Therefore, we use Complex Programmable Logic Device (CPLD) which has both characteristics of the software program and the logic circuit for the mixing device.

Figure 10 The image of flight experiment.

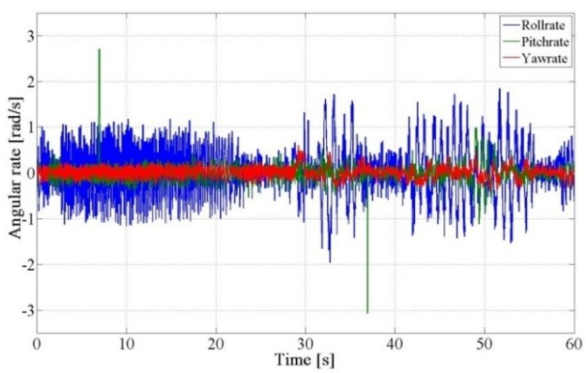

(a) Angular velocity

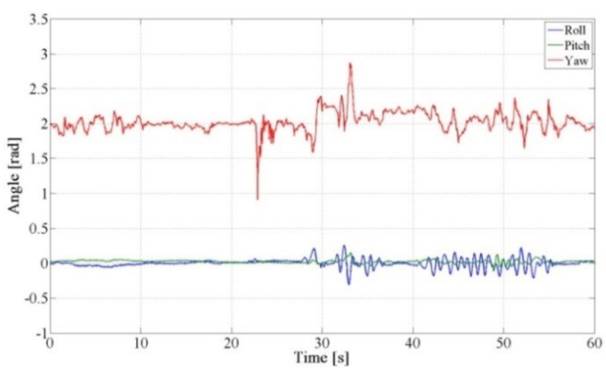

(b) Attitude

Figure 11 Flight data in the experiment.

B. Flight Experiment

A flight experiment was carried out by using abovementioned control system. The image of the flight experiment is shown in **Figure 10**. Moreover, the flight data obtained by the control device are shown in **Figure 11**. In **Figure 11**, top figure shows the angular velocity and bottom figure shows the attitude of the helicopter. By using the flight data, the parameters in the mathematical model could be identified.

V. CONCLUSION

In this paper, the intermeshing quadrotor helicopter which has both characteristics of tandem rotor helicopter and intermeshing rotor helicopter was proposed. For motion analysis of the intermeshing quadrotor helicopter, the nonlinear mathematical model was derived using the velocity transformation method. The model including the rotor flapping dynamics was successfully derived. All the forces and moments generated by rotors are derived by using the blade element theory. Finally, the control system for flight experiment was developed, and the flight experiment by manual operation was carried out for collecting the flight data.

In future works, the model parameters which need parameter identification such as rotor aerodynamic parameters are identified using the flight data. Then the fundamental motion analysis is conducted to show the motion characteristics of the intermeshing quadrotor helicopter. And finally, the autonomous control system is designed utilizing the characteristics obtained from the analysis.

ACKNOWLEDGMENT

This work was supported by JSPS KAKENHI Grant Number 24760185.

REFERENCES

[1] B. Mettler, M. B. Tischler, and T. Kanade, "System Identification Modeling of a Small Scale Unmanned Rotorcraft for Flight Control Design," *Journal of American Helicopter Society*, vol. 47, no. 1, 2002, pp. 50–63. CrossRef

[2] C. Bermes, S. Leutenegger, S. Bouabdallah, D. Schafroth, and R. Siegwart, "New Design of the Steering Mechanism for a Mini Coaxial Helicopter," *Proceedings of IEEE International Conference on Intelligent Robots and Systems*, Nece, France, 2008, pp.1236-1241. CrossRef

[3] J. H. Lee, B. M. Min, and E. T. Kim, "Autopilot Design of Tilt-rotor UAV using Particle Swarm Optimization Method," *Proceedings of International Conference on Control, Automation and Systems 2007*, Seoul, Korea, 2007, pp. 1629–1633. CrossRef

[4] S. Shen, N. Michael, and V. Kumar, "Autonomous Milti-floor Indoor Navigation with a Computationally Constrained MAV," *Proceedings of IEEE International Conference on Robotics and Automation*, Shanghai, China, 2011, pp. 20-25. CrossRef

[5] H. Tajima, *Fundamental of Multibody Dynamics*, Tokyo Denki University Press, 2006, (in Japanese).

[6] A. A. Shabana, *Dynamics of Multibody Systems, 3rd Edition*, Cambridge, 2005.

[7] W. Jekkovsky, "The Structure of Multibody Dydnamics Equations," *Journal of Guidance, Control, and Dynamics*, vol. 1, no. 3, 1978, pp.173-182. CrossRef

[8] S. S. Kim, and M. J. Vanderploeg, "A General and Efficent Method for Dynamics Analysis of Mechanical System Using Velocity Transformation," *ASME Journal of Mechanisms, Transmissions, and Automation Design*, vol. 108, 1986, pp. 176-182. CrossRef

[9] A. R. S. Bramwell, G. Done, and D. Balmford, *Bramwell's Helicopter Dynamics*, 2nd Edition, Butterworth-Heinemann, 2001.